Electronic structure of the energetic material 1,3,5-triamino-2,4,6-trinitrobenzene

S. Kakar*
Department of Applied Science, University of California at Davis/Livermore, Livermore, California 94550

A. J. Nelson†
Chemistry and Materials Science Directorate, Lawrence Livermore National Laboratory, Livermore, California 94550

R. Treusch
Department of Physics, University of Wisconsin, Madison, Wisconsin 53706

C. Heske
Advanced Light Source, Lawrence Berkeley National Laboratory, Berkeley, California 94720

T. van Buuren, I. Jiménez,‡ P. Pagoria, and L. J. Terminello
Chemistry and Materials Science Directorate, Lawrence Livermore National Laboratory, Livermore, California 94550
(Received 15 March 2000)

Synchrotron radiation is used to study the electronic structure of the energetic material 1,3,5-triamino-2,4,6-trinitrobenzene (TATB). Element and site-specific density of unoccupied electronic states in TATB is probed by x-ray-absorption spectroscopy at the C, N, and O *K* edges. In addition to illuminating the electronic structure of TATB, the absorption data enable the understanding of microscopic changes occurring in such compounds due to various damage mechanisms. The absorption data are further supplemented by data from the core-level and valence-band photoelectron spectroscopy of thin films of TATB.

I. INTRODUCTION

Energetic materials are substances that undergo exothermic chemical reaction in response to an external stimulus.[1] This response takes place on time scales ranging from milliseconds to femtoseconds and leads to combustion, explosion, or detonation of the material depending on the time of reaction, the energy released, and initiation process.[2,3] These materials are among the earliest of the man-made classes of materials and perhaps among the most important. Their applications are wide and varied, and in some cases indispensable. To name a few, they are used as propellants, blasting agents, pyrotechnics, gas inflators, and for military purposes. It is then not surprising that the creation of new and safer energetic materials that are optimally suited to their use is a central problem in energetic materials science.[3] It is the purpose of this paper to probe the electronic structure of a widely used energetic material to attribute the well-known properties of the material to the intricacies of its fundamental structure. Only with such an understanding at a microscopic level can the hope of a rational synthesis of energetic materials be realized.

We have measured the electronic structure of the widely used prototype energetic material 1,3,5-triamino-2,4,6-trinitrobenzene (TATB) (schematically sketched in Fig. 1) using x-ray absorption spectroscopy (XAS) and core-level and valence-band photoelectron spectroscopy (VBPES). XAS data are obtained at the *K* edges of C, N, and O and these data probe the unoccupied orbitals of the molecule. VBPES, on the other hand, probes the occupied electronic states and hence, together with XAS provides detailed information about the electronic structure of the material.

The potential utility of the aforementioned spectroscopic data is explained as follows. Most energetic materials consist of molecular units containing C, N, O, and H atoms.[3] Theoretical calculations show that the spatial arrangements and steric configurations of specific molecular units, that include C-NO_2, N-O, N-H, and C-NH_2, ultimately determine the performance of energetic materials.[3,4] For this reason, the synthesis of new energetic materials often involves choosing molecular constituents having particular atomic geometry and local chemical environments so as to promote the performance of materials in the desired direction.[3] However, a comprehensive predictive model suitable for this purpose is still under development. Clearly a microscopic understanding of the local chemical environment of individual atoms in known energetic materials can be helpful in creating such a model. XAS is an ideal tool for this purpose as it has the

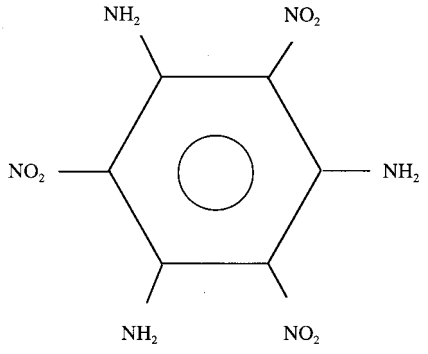

FIG. 1. Planar view of 1,3,5-triamino-2,4,6-trinitrobenzene (TATB).

ability to select atoms of a given elemental species in a sample and excite their spatially localized core electrons to unoccupied electronic states. This elemental and site specificity makes the technique a powerful probe of the bonding between the excited atom and its neighbors.[5] Furthermore, the information so obtained can be used in conjunction with the VBPES to decipher both occupied and unoccupied electronic states of the species and hence, the electronic excitations between the two. The latter information is valuable as it may help to determine important properties of energetic materials such as their sensitivity, damage threshold, and response to shock initiation. In addition, these data can provide spectroscopic fingerprints of energetic materials, which can be useful for noninvasive identification of even minute quantities of these materials, as well as for studying the effects of various damage mechanisms (e.g., aging, shock, heat, radiation, or chemical) on these materials. To illustrate this point, we performed a XAS study of a radiation-damaged TATB sample. The results of this study clearly demonstrate how the comparison of the spectroscopic data from a post-damage residue and a control sample makes it possible to relate the damage mechanism to changes in individual chemical species or bonds in the material and hence, glean important information regarding its performance and limitations.

II. EXPERIMENT

The XAS and PES experiments were performed at the Stanford Synchrotron Radiation Laboratory (SSRL), Stanford, CA and repeated at ALS for reference energy calibration purposes (see below). Monochromatized synchrotron radiation from the spherical grating monochromator equipped beamline 8-2 (Ref. 6) was used to excite TATB, which was deposited by thermal evaporation on a Si wafer. TATB was commercially available and had a purity of 98%. The Si wafer was flashed prior to the deposition and XAS was used to make certain there were no C, N, or O containing residues on the wafer. The thickness of evaporated TATB films was estimated to be a few 1000 Å. X-ray photoabsorption was measured as a function of the excitation energy in the vicinity of the K edges of C, N, and O by monitoring total-electron-yield in the relevant energy range[5] with a monochromator energy resolution of $\Delta E \approx 150$ meV. Core-level photoelectrons from the sample were collected by a cylindrical mirror analyzer operated in an angle-integrated mode to yield photoelectron intensity as a function of kinetic energy. Chemical changes in TATB molecules induced by evaporation were discounted by comparison of XAS spectra for the thin films with those for TATB powder. Measurements were also taken for several angles of incidence of the exciting radiation to decipher any angular dependence in the spectra and thus any implicit structural order in the deposited films. The measurements were also repeated as a function of time to discount any radiation-induced damage of the sample. The energy of the synchrotron radiation was calibrated by determining energy positions of known spectral features in the simultaneously recorded x-ray absorption spectra of highly ordered pyrolytic graphite,[7] BN,[8] and SiO_2 (Ref. 9) at the K edges of C, N, and O, respectively. In addition, we probed the radiation-induced damage of TATB molecular films by performing similar measurements on a thin film exposed to intense nonmonochromatized radiation for varying lengths of time as described below.

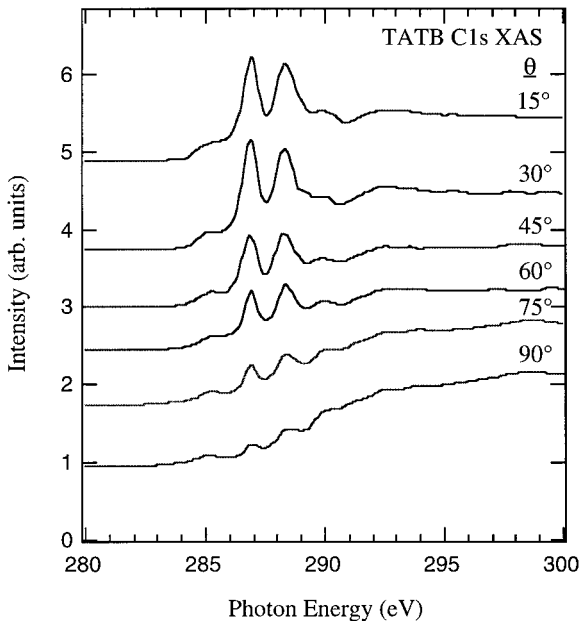

FIG. 2. C 1s absorption spectra for TATB for various angles of incidence θ, of synchrotron radiation measured with respect to the sample surface.

The VBPES data were obtained at the beamline 8.0 (Ref. 10) at the Advanced Light Source, Lawrence Berkeley National Laboratory, Berkeley, CA and repeated at SSRL for reference energy calibration purposes. The spherical grating monochromator was operated to deliver radiation of energy $h\nu = 240$ eV to photoionize TATB films prepared as explained above. The resulting photoelectrons from the sample were collected by an ellipsoidal-mirror analyzer operated in an angle-integrated mode to yield photoelectron intensity as a function of kinetic energy.[11] The combined energy resolution of the monochromator and the analyzer was $\Delta E \approx 200$ meV. The Fermi energy position was determined from the Ta metal clips in contact with the sample. Since the incident photon intensity is very high at this source, it was essential to minimize the exposure of the sample to the radiation to prevent damage.

III. RESULTS AND DISCUSSION

A. C 1s absorption spectra

Figure 2 shows C 1s spectra measured as a function of the incidence angle in the energy range 280–300 eV. All spectra have been normalized to the same edge jump by equalizing baselines below the edge, then equalizing intensities well above the edge by a multiplicative factor.[5] The prominent features in these spectra are the peaks at 286.8 and 288.3 eV. These correspond to transitions from the C 1s core level to the unoccupied π^* orbitals of the TATB molecule. The features relate to two distinct environments of C atoms in the molecule, namely, the aromatic C atoms attached to the -NH_2 and -NO_2 moieties. The strongly polarized -NO_2 ligand withdraws mobile π electrons from the ring $\pi_{C=C}$ system, which would normally result in a strong chemical shift to higher

TABLE I. Summary of x-ray absorption peak energies and bonding assignments for TATB.

Absorption edge	Peak energy (eV)	Bond assignment
C *K* edge	285.2	C-H
	286.8	C-NO_2
	288.3	C-NH_2
	289.6	C-O
N *K* edge	398.0	N-H
	402.5	N-O
O *K* edge	530.3	O-N
	537.7	O-C

photon energies for the C $1s$ (C-NO_2)$\rightarrow\pi^*_{C=C}$ transition.[4,12–14] However, in a TATB molecule this picture is radically altered by the presence of -NH_2 substitutes in the ring. Although also electronegative, the N atom in the -NH_2 ligand is basic, i.e., an electron pair donor, and it tends to share its lone pair of electrons with the electron-deficient ring and acquire a positive charge.[15] As a result, the contribution to the C $1s$ (C-NO_2) chemical shift arising from strong polarization of the -NO_2 substituent is effectively negated. On the other hand, the C $1s$ (C-NH_2)$\rightarrow\pi^*_{C=C}$ transition is shifted to higher photon energies due to the reduced negative charge around C atoms bonded to -NH_2 groups. Note that in TATB each -NO_2 group can effectively attract at most two electrons from the ring, which is the same as the number of electrons available to the ring from the -NH_2 group. Based on this simple picture, the low-energy feature at 286.8 eV can be attributed to excitations localized on the C atoms attached to -NO_2 groups, and the high-energy feature at 288.3 eV to those occurring on C atoms attached to -NH_2 groups. These results are summarized in Table I. Thus we see that the details of C $1s$ absorption spectra provide an insight into the donor-acceptor electronic interactions between the -NH_2 and -NO_2 groups through their influence on the C $2p$ contributions to the π^* orbitals. It is interesting to note that the $1s$ (C-NO_2)$\rightarrow\pi^*_{C=C}$ transition in TATB occurs approximately at the same photon energy as the C $1s$ (C-NH_2)$\rightarrow\pi^*_{C=C}$ transition in $C_2H_5NH_2$.[16] On the other hand, the C $1s$ (C-NH_2)$\rightarrow\pi^*_{C=C}$ transition energy for TATB is higher than for the same transition in $C_2H_5NH_2$.[16] These observations are consistent with the qualitative arguments outlined above.

Figure 2 also shows that the intensity of the $\pi^*_{C=C}$ resonances depends strongly on the angle of the incidence θ, of the exciting radiation with respect to the sample plane. The resonances are strong at a grazing x-ray incidence and diminish as the incidence tends to normal. Owing to the linearly polarized nature of synchrotron radiation and the experimental arrangement used in this paper, this observation points to an ordering of TATB molecules on the substrate.[5] If the six-membered rings of carbon atoms all lie flat on the surface with their π^* orbitals oriented along the surface normal, an enhancement in resonant behavior would be observed when the exciting electric field vector has a large projection along the direction of π^* orbitals, i.e., at grazing angles of incidence.[5] This observation is consistent with the nearly perfect cleavage plane exhibited by triclinic TATB crystals and its pleochroic properties, as well as the results of crystal structure calculations.[4,17] Specifically, calculations with larger basis sets and gradient corrected density-functional theory (DFT) indicate that TATB is very nearly planar.[4]

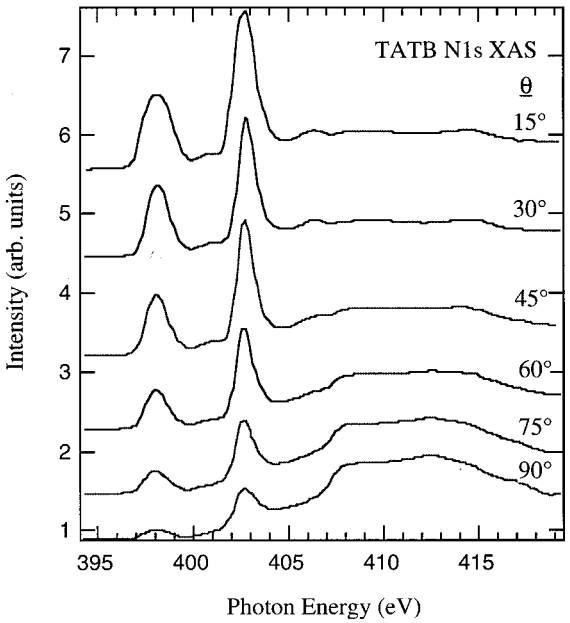

FIG. 3. N $1s$ absorption spectra for TATB for various angles of incidence θ, of synchrotron radiation measured with respect to the sample surface.

There are additional features in the above spectra worth noting. Some of these features, e.g., the peak at 285.2 eV, show no angular dependence and they probably arise due to carbon-based impurities present in our sample. The peak at 289.6 eV shows minimal polarization dependence and may be associated with C-O impurities. However, it is difficult to interpret their origins solely based on qualitative arguments. A detailed interpretation of these features will require a sophisticated theoretical treatment taking into account the multiconfigurational states of the molecule, the effect of core-hole localization, and the solid-state effects such as the strong intermolecular hydrogen bonding.[4,17] For this reason, we have chosen to focus our attention here, and in subsequent absorption spectra, only on the strongest and bond order significant spectral features. Finally, we also neglect the continuum region at high energies. This energy region is dominated by broad overlapping σ^* resonances corresponding to various bonds of the core-excited atom in the TATB molecule, which makes any qualitative gleaning of information difficult. Moreover, in contrast to the π^* resonances, which can serve as the fingerprint of the local bonding environment, σ^* states can contain contributions from photoelectron scattering processes involving distant neighbors resulting in loss of correlation with local bonding.[5]

B. N 1*s* absorption spectra

Figure 3 shows N $1s$ spectra measured as a function of the incidence angle in the energy range 394–419 eV. The spectra show two prominent peaks at 398.0 and 402.5 eV. For the assignment of these peaks we note that the -NO_2

group in TATB has an unoccupied π^*_{NO} orbital. For this reason the N $1s$ (C-NO_2)$\rightarrow\pi^*_{NO}$ transition is expected to be quite intense since both the initial and the final states involved in the transition lie in the same spatial region. Hence, we attribute the high-energy peak to N $1s$ (C-NO_2)$\rightarrow\pi^*_{NO}$ excitations. The origin of the low-energy feature, however, is less obvious. Unlike the -NO_2, the -NH_2 group has essentially a saturated character, which should give rise only to a weak Rydberg structure in this energy region. This is in fact the behavior exhibited by compounds such as CH_3NH_2 (Ref. 18) and $C_2H_5NH_2$.[16] However, calculations for x-ray absorption spectra of disubstituted nitroanilines indicate that the $\pi^*_{C=C}$ and π^*_{NO} orbitals in a TATB molecule are sufficiently delocalized to have a nonzero amplitude over the -NH_2 group.[16] This makes possible the transitions from N $1s$ (C-NH_2) core level to mixed $\pi^*_{C=C}/\pi^*_{NO}$ states.[16] We attribute the low-energy peak at 398.0 eV to these phenomena as summarized in Table I. Note that this peak has larger full width at half maximum than the N $1s$ (C-NO_2)$\rightarrow\pi^*_{NO}$ feature, which probably is a reflection of the mixing of orbitals. Overlapping orbitals may also be the cause of the broadening of the $1s$ (C-NO_2)$\rightarrow\pi^*_{C=C}$ peak discussed above. Further evidence supporting this assignment comes from the bond order calculations of Cady *et al.*, that give a value of 1.46 for the carbon-nitrogen bond for the amine group (in contrast to 1.02 for the nitro group).[17] Also of interest here is the 4.5 eV energy separation between the two transitions. This compares with a 6.0 eV difference in N $1s$ (C-NO_2) and N $1s$ (C-NH_2) binding energies obtained from our photoemission measurements. Previous x-ray photoemission spectroscopy (XPS) studies of TATB (Refs. 19 and 20) yield a 5.6 eV energy separation in good agreement with our measurements. However, the discrepancy of 1.5 eV highlights another important feature related to the donor-acceptor nature of the TATB molecule. Owing to differences in charge distributions, a N $1s$ core hole belonging to the -NH_2 moiety (donor) is shielded differently from the excited electron as compared to a N $1s$ core hole on the -NO_2 moiety (acceptor). This produces a site-dependent shift in the respective final states of excitation, which then must be added to the initial-state shift due to chemical bonding to determine transition energies.[5,21,22] The magnitudes of these two contributions to observed transition energies cannot be decoupled experimentally and can be estimated only by theoretical means. Finally, we note that the N $1s$ absorption spectra show similar angular dependence as observed in the C $1s$ absorption spectra, indicating again the flat and oriented nature of TATB molecules on the substrate, including the nitrogen containing moieties, as predicted by recent theoretical calculations.[4]

C. O 1*s* absorption spectra

Figure 4 shows the O $1s$ absorption spectra in the energy range 520–555 eV. The strong peak at 530.3 eV corresponds to the O $1s\rightarrow\pi^*_{NO}$ orbitals. The broad feature with peak energy at 537.7 eV is due to σ^* orbitals and exhibits minimal polarization dependence. These results are summarized in Table I. As in the case of the C $1s$ and N $1s$ absorption spectra, these spectra also reflect an ordered arrangement of TATB molecules in the sample and testify to their planar nature.[4] Our photoemission measurements yield an O $1s$ core-level bonding energy of 531.6 eV in agreement with previous XPS studies of TATB.[19,20]

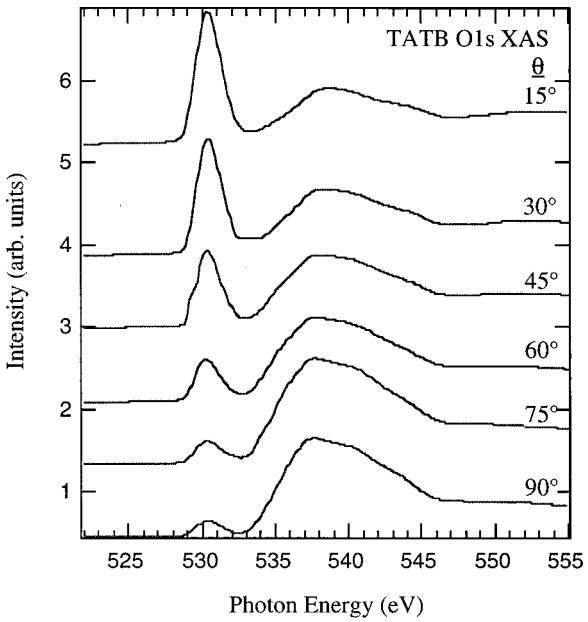

FIG. 4. O $1s$ absorption spectra for TATB for various angles of incidence θ, of synchrotron radiation measured with respect to the sample surface.

D. Radiation damage

Figure 5 compares the N $1s$ x-ray absorption spectrum for a freshly prepared film of TATB molecules (bottom curve) with those for a TATB film exposed to varying doses of radiation (white light from the bend magnet beamline at SSRL). Data were obtained after irradiation of the sample for

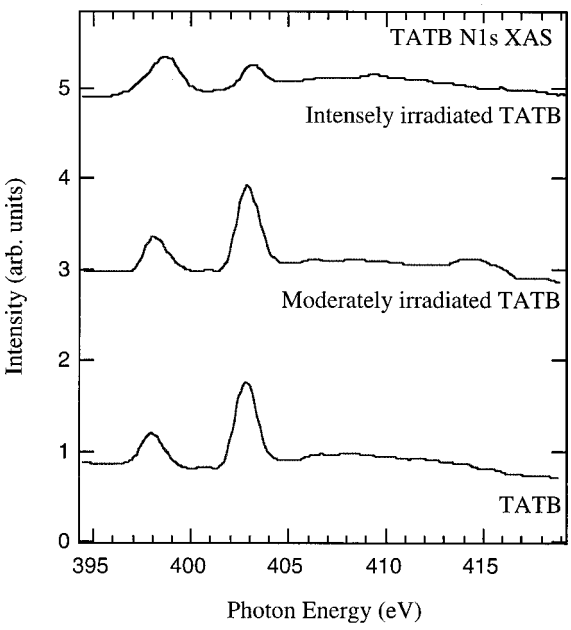

FIG. 5. N $1s$ absorption spectra for TATB; bottom—A fresh TATB film; middle—TATB film exposed to moderate dose of radiation for 5 min; top—TATB film exposed to intense dose of radiation for 5 min.

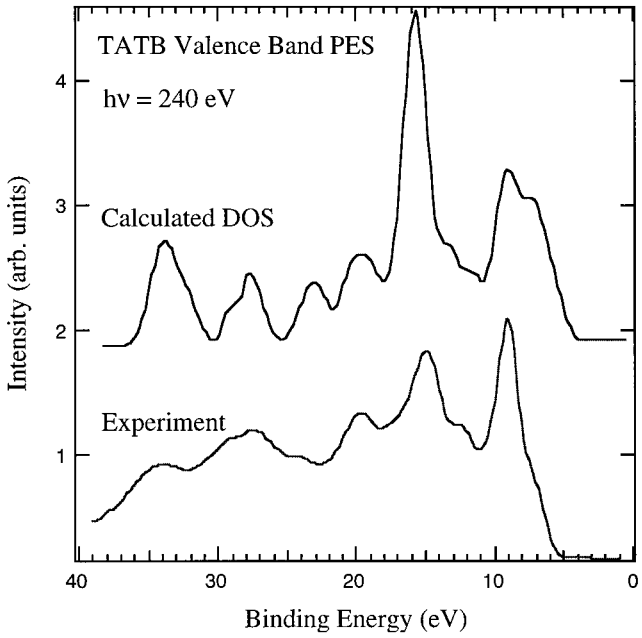

FIG. 6. Comparison of calculated DOS (Ref. 1) and experimental valence-band photoemission spectrum for TATB at $h\nu = 240$ eV.

5 min with moderately intense radiation (ca. 10^{10} photons/s, middle curve) and for 5 min. with very intense radiation ($\sim 10^{14}$ photons/s, top curve). There are clear trends observed in these spectra, which allow an unambiguous deciphering of the response of the TATB molecule to radiation. As illustrated, the molecule is able to withstand a moderate irradiation as no appreciable change in absorption is observed after such an event. Heavy dosage, on the other hand, significantly alters the absorption of the sample. Whereas the intensity of the transitions originating from -NH_2 remains unaltered, the N $1s$ (C-NO_2)$\rightarrow \pi^*_{NO}$ transition undergoes severe attenuation. This effect is also observed in the C $1s$ and O $1s$ spectra (not shown), where the C $1s$ (C-NO_2)$\rightarrow \pi^*_{C=C}$ and O $1s \rightarrow \pi^*_{NO}$ transitions exhibit a corresponding depletion of strength. These observations imply a change in the molecular composition. Specifically, the response of the TATB molecule to an intense radiation stimulus is to eject the -NO_2 substituent from the ring. This is consistent with the observation that the loss of the nitro group (NO_2) is the primary event in the initial stages of TATB decomposition.[19] Another manifestation of this effect is the broadening of the peak corresponding to the N $1s$ (C-NH_2)$\rightarrow \pi^*_{NO}$ transition; due to the partial loss of the -NO_2 groups from the molecule, the three -NH_2 sites are no longer equivalent. These observations clearly bring forth the utility of core-level spectroscopy as an analytical tool for determining bonding and chemical changes in energetic materials due to aging or other damage mechanisms.

E. Valence-band photoelectron spectrum

Figure 6 shows the valence-band photoelectron spectrum for TATB at incident photon energy equal to 240.0 eV. The data are shown subsequent to background subtraction[23] and the position of the valence-band maximum is 5.8 eV below the Fermi energy (E_F). The observed spectral features correspond to the highest occupied molecular orbitals (HOMO's) of TATB, which include molecular orbitals on the aromatic ring, molecular orbitals on the lone pairs of the amino nitrogens, and molecular orbitals on the -NO_2 groups. There are 96 valence electrons in a TATB molecule and as a result, the assignment of spectral features in the valence-band photoelectron spectrum to specific bond/moiety in the molecule is a nontrivial task.[19,24] Clearly the observed features consist of many overlapping orbitals, which precludes such an assignment. However, Kunz has used *ab initio* methods to calculate the total density of electronic states (DOS) for solid TATB,[1] which can be directly compared with our data. For this purpose, we have modified the theoretical DOS by convoluting it with Gaussian peaks of width $\sim$1.6 eV to account for experimental and solid-state broadening. Furthermore, the theoretical results are shifted by 1.6 eV to lower binding energy for the best match with experimental results; the determination of the exact position of zero on the energy scale is difficult theoretically due to potential inadequacies in models. The results of this procedure, presented in the top section of Fig. 6, show an excellent qualitative agreement with experimental data. The calculated DOS reproduces both the shape and the sequence of observed spectral features. The differences in relative intensities of various features, such as those at 7.4, 14.9, and 24.3 eV, probably arise from the modulating effect of the dipole matrix element.[25] Minor discrepancies are also observed for the energy separation between some of the peaks; these can be attributed to various approximations made in the theoretical treatment, e.g., the neglect of correlation effects.[1]

F. Estimation of the band gap

The donor-acceptor nature of a TATB molecule indicates that in its neutral state the molecule has its HOMO localized on the six-membered ring and the -NH_2 group (donor), while the lowest unoccupied molecular orbital (LUMO) is localized on the -NO_2 group (acceptor). Also, as a first approximation, the HOMO-LUMO gap or band gap must be in the range of 4.9–7.2 eV, the energy gaps for benzene and *p* nitroaniline, respectively. The energy position of the N $1s$ (C-NO_2)$\rightarrow \pi^*_{NO}$ transition can be used to determine the LUMO energy in the *core-excited* molecule. This is the energy position of the transition minus the N $1s$ (C-NO_2) ionization potential (404.6 eV) for TATB measured using XPS,[16] and is equal to -2.1 eV. This number can be used to estimate the LUMO energy in the *neutral* molecule by considering the effect of the N $1s$ (C-NO_2) core hole on the unoccupied molecular orbitals. Upon core-hole creation, the LUMO is pulled down in energy due to Coulombic attraction exerted by the core hole. The magnitude of this effect is directly related to the changes in the electron distribution as electrons from everywhere on the ring are pulled to the ionized atom to screen the core hole; it must be determined in order to obtain the LUMO energy for the neutral molecule. This is a nontrivial task amenable only to sophisticated theoretical treatments. Though no such treatment exists for TATB, it is possible to find the corresponding results for a similar molecule *p*-nitroaniline (H_2N-C_6H_5-NO_2 with -NO_2 and -NH_2 groups located diametrically opposite to each other

on the phenyl ring).[26] Freund *et al.* have calculated the effect of core-hole screening in N 1*s* (C-NO_2) photoionization of *p* nitroaniline and found that in this case, the LUMO is pulled down in energy by 6.7 eV while the HOMO is only pulled down 3.8 eV thus decreasing the HOMO-LUMO energy gap from 7.1 eV for the neutral molecule to 4.3 eV for the N 1*s* (NO_2) molecule, a difference of 2.8 eV. We use these numbers as an estimate of the core-hole-electron excitation in TATB to arrive at the LUMO energy of 4.6 eV in the neutral molecule. Applying the same formalism to the HOMO energy (-5.8 eV from Fig. 6) determined from VBPES, we arrive at the HOMO energy of -2.0 eV in the neutral molecule. Therefore, the band or the HOMO-LUMO energy gap can be estimated to be 6.6 eV in neutral TATB. This is in comparison to the complete active space multiconfiguration self-consistent field (CASSCF) calculations by Wu *et al.* that yield a band-gap range of 4.6 eV to 5.7 eV.[27] In view of the qualitative and approximate approach adopted here, this is a rather satisfactory result.

IV. CONCLUSIONS

C, N, and O *K*-edge photoabsorption data were obtained for the energetic material TATB. These data probe the chemical bonding environment in the molecule with site specificity, and exhibit features that can be correlated to -NH_2 and -NO_2 ligands of the molecule. The results illuminate the important role of intramolecular charge transfer in determining the electronic structure of donor-acceptor molecules such as TATB. The net transfer of negative charge from the basic -NH_2 group to the highly electronegative -NO_2 group in the TATB molecule dramatically affects the assignment of transitions in the absorption spectra through changes in the core-level binding energies of C and N atoms. We also find observed spectral features to vary with the angle of incidence of the polarized exciting radiation; this indicates an ordered growth mechanism wherein the TATB molecules arrange themselves coplanar with the orientation of the surface. We aim to further use this technique to study energetic materials of a diverse kind. The database so created will help in discerning trends that can provide a much-needed basis for theoretical understanding of energetic materials at a microscopic level. In the same vein, we have obtained valence-band photoemission data for TATB and have used them in conjunction with the XAS data to arrive at an estimate of 6.6 eV for the band gap of TATB. Moreover, we have compared these results with the results of *ab initio* calculations of the total density of occupied and unoccupied electronic states and total-energy CASSCF calculations for the band gap of solid TATB. The agreement obtained is encouraging and should motivate similar theoretical efforts for other energetic materials.

Finally, the results of this paper also bear relevance to applied materials science. The spectroscopic fingerprints, such as those found in this paper, provide means to track chemical changes in energetic materials on exposure to various external stimuli. As an example, this paper demonstrates that exposures of TATB to intense radiation, lead to the ejection of -NO_2 groups from the TATB molecule, thereby seriously impairing its performance as an energetic material. Such information can be of paramount importance in the synthesis and characterization of new energetic materials.

ACKNOWLEDGMENTS

We would like to thank the SSRL and ALS staff for their assistance during these experiments. Work was supported by the Director, Office of Energy Research, Office of Basic Energy Sciences, and was performed under the auspices of the U.S. Department of Energy by University of California, Lawrence Livermore National Laboratory, under Contract No. W-7405-ENG-48. This work was conducted at the Stanford Synchrotron Radiation Laboratory and the Advanced Light Source at Lawrence Berkeley National Laboratory, which are supported by the U.S. Department of Energy under Contract Nos. DE-AC03-76SF00515 and DE-AC03-76SF00098, respectively.

*Present address: Lucent Technologies, Norcross, GA 30071.
†Corresponding author.
‡Present address: Dept. Intercaras y Crecimiento, ICMM-CSIC, Campus de Cantoblanco, E-28049 Madrid, Spain.

[1] A. B. Kunz, Phys. Rev. B **53**, 9733 (1996).
[2] *Chemistry and Physics of Energetic Materials*, edited by S. N. Bulusu (Kluwer Academic, Dordrecht, 1990).
[3] *Structure and Properties of Energetic Materials*, edited by D. H. Liebenberg, R. W. Armstrong, and J. J. Gilman, Mater. Res. Soc. Symp. Proc. No. 296 (Materials Research Society, Pittsburgh, 1993).
[4] C. J. Wu and L. E. Fried, J. Phys. Chem. **A104**, 6447 (2000).
[5] J. Stöhr, *NEXAFS Spectroscopy* (Springer-Verlag, Berlin, 1992).
[6] K. G. Tirsell and V. Karpenko, Nucl. Instrum. Methods Phys. Res. A **291**, 511 (1990).
[7] E. J. Mele and J. J. Ritsko, Phys. Rev. Lett. **43**, 68 (1979).
[8] I. Jimenez, A. F. Jankowski, L. J. Terminello, D. G. J. Sutherland, J. A. Carlisle, G. L. Doll, W. M. Tong, D. K. Shuh, and F. J. Himpsel, Phys. Rev. B **55**, 12 025 (1997).
[9] N. Brun, C. Colliex, J. Rivory, and K. Yu-Zhang, Microsc. Microanal. Microstruct. **7**, 161 (1996).
[10] J. J. Jia, T. A. Calcott, J. Yurkas, A. W. Ellis, F. J. Himpsel, M. G. Samant, J. Stöhr, D. L. Ederer, J. A. Carlisle, E. A. Hudson, L. J. Terminello, D. K. Shuh, R. C. C. Perera, Rev. Sci. Instrum. **66**, 1394 (1995).
[11] D. E. Eastman, J. J. Donelson, N. C. Hien, and F. J. Himpsel, Nucl. Instrum. Methods **172**, 327 (1980).
[12] K. Siegbahn, C. Nordling, G. Johansson, J. Hedman, P. F. Heden, K. Hamrin, U. Gelius, T. Bergmark, L. O. Werme, R. Manne, and Y. Baer, *ESCA Applied to Free Molecules* (North-Holland, Amsterdam, 1969).
[13] R. McLaren, S. A. C. Clark, I. Ishii, and A. P. Hitchcock, Phys. Rev. A **36**, 1683 (1987).
[14] M. B. Robin, I. Ishii, R. McLaren, and A. P. Hitchcock, J. Electron Spectrosc. Relat. Phenom. **47**, 53 (1988).
[15] R. T. Morrison and R. N. Boyd, *Organic Chemistry* (Allyn and Bacon, Boston, 1983), pp. 616.
[16] C. C. Turci, S. G. Urquhart, and A. P. Hitchcock, Can. J. Chem. **74**, 851 (1996).
[17] H. C. Cady and A. C. Larson, Acta Crystallogr. **18**, 485 (1965).

[18] R. N. S. Sodhi and C. E. Brion, J. Electron Spectrosc. Relat. Phenom. **36**, 187 (1985).
[19] J. Sharma, W. L. Garrett, F. J. Owens, and V. L. Vogel, J. Phys. Chem. **86**, 1657 (1982).
[20] J. Sharma, B. C. Beard, and M. Chaykovsky, J. Phys. Chem. **95**, 1209 (1991), private communication.
[21] E. W. Plummer, W. R. Salanek, and J. S. Miller, Phys. Rev. B **18**, 1673 (1978).
[22] H.-J. Freund and E. W. Plummer, Phys. Rev. B **23**, 4859 (1981).
[23] D. A. Shirley, Phys. Rev. B **5**, 4709 (1972).
[24] P. C. Hariharan, W. S. Koski, J. Kaufman, and R. S. Miller, Int. J. Quantum Chem. **XXIII**, 1493 (1983).
[25] B. H. Bransden and C. J. Joachain, *Introduction to Quantum Mechanics* (Longman Scientific and Technical, Essex, 1989), pp. 425.
[26] H.-J. Freund and R. W. Bigelow, Phys. Scr. **T17**, 50 (1986).
[27] C. Wu (to be published).